

Methods

Experimental design and electroformation

Amphotericin B (AmB), dimethyl sulfoxide (DMSO), sodium dithionite ($\text{Na}_2\text{S}_2\text{O}_4$), tricine, 1,2-dipalmitoyl-sn-glycero-3-phosphocholine (DPPC), fluorescein and ergosterol (ERG) were obtained from Sigma Aldrich. 1-palmitoyl-2-oleoyl-glycero-3-phosphocholine (POPC) was purchased from Avanti Polar Lipids Inc. Hydrochloric acid (HCl), ethanol, 2-propanol, potassium chloride (KCl) and chloroform were purchased from POCH. Water used in all experiments was purified by a Milli-Q system from Merck Millipore. Amphotericin B was purified as described previously.⁵⁰ Giant unilamellar liposomes (GUV) were formed from DPPC or POPC with addition of either AmB or AmB and ergosterol (30% mol of ergosterol with respect to the phospholipid) using the electroformation technique.⁵¹ Platinum electrodes covered with dried lipids were placed in a cuvette containing water with 30 mM KCl and $8.6 \cdot 10^{-6}$ M fluorescein (pH 8.0). Liposome electroformation was carried out for 2 h (AC sinusoidal field, 10 Hz, 3 V). AmB in a DMSO solution was added to water after 1 h of electroformation. The final AmB concentration was 0.5% mol or 0.05% mol with respect to the phospholipid. During electroformation, temperature was maintained at 45°C or 30°C, i.e. above the main phase transition respectively of DPPC or POPC. The final concentration of DMSO in the liposome suspensions was 0.15%. During microscopy measurements 2 μl of 0.7% HCl was added to the 50 μl liposome solution.

Dithionite bleaching assay of AmB interleaflet equilibration

For measurements of AmB equilibration between the two leaflets of a lipid membrane, GUVs were formed in the buffer solution (20mM Tricine, 10mM KCl, pH 7.6) using the method described above. In the two variants of the experiment, AmB in DMSO was added to the buffer either during or after electroformation, corresponding to two- or one-sided addition of the drug, respectively. 30 minutes after GUV formation/AmB addition, 2 μl of freshly prepared $\text{Na}_2\text{S}_2\text{O}_4$ solution (10 mg/ml) was added to the 50 μl liposome dilution and a series of microscopic observations of fluorescence intensity were performed in 2-minute intervals.

Steady state and time resolved measurements

Absorption spectra were recorded with a Cary 60 UV-VIS spectrophotometer (Agilent Technologies). The concentration of AmB was established based on the molar extinction coefficient ($121400 \text{ M}^{-1} \cdot \text{cm}^{-1}$) at 416 nm, corresponding to an absorption maximum in DMSO solution.⁵²

Microscopy data was recorded on a MicroTime 200 confocal system from PicoQuant GmbH, connected to an Olympus IX71 inverted microscope. The samples were excited with pulsed lasers working at a 10 MHz repetition rate. In all experiments a silicon-immersed objective (Olympus NA = 1.3, 60) was used. The observation was performed in the confocal configuration using a 50- μm diameter pinhole, with optic filters used depending on the experiment. For AmB imaging a 405 nm solid-state laser was used, and fluorescence was monitored with a ZT 405RDC dichroic filter, ZET405 StopLine Notch Filter and a 430 nm pass filter (all pur-

chased from Chroma-AHF Analysentechnik). Fluorescein lifetime was imaged with a 440 nm excitation laser line, and observation was performed through SDDC440 dichroic and 520/35 band pass filters (both from Chroma-AHF Analysentechnik). Fluorescence lifetimes data was analyzed using the SymPhoTime 64 v. 2.3 software (PicoQuant). Fluorescein lifetime calibration as a function of pH was carried out using a FluoTime 300 spectrometer (PicoQuant) (see Fig. S1b,c). Data was obtained using a 405 nm laser and a repetition rate of 20 MHz. Fluorescence emission intensity decays were recorded in the 510-530 nm wavelength range, and were fitted with four exponential components⁵³ according to formula below:

$$I(t) = \sum_i \alpha_i e^{-\frac{t}{\tau_i}} \quad (1)$$

where α_i is the relative amplitude of the component and τ_i is the decay time.

Molecular models

To examine the properties of AmB oligomers in lipid bilayers of different composition, we performed Molecular Dynamics (MD) simulations in 3 membrane systems models, consisting of: (a) pure dipalmitoylphosphatidylcholine (DPPC), referred to as DPPC; (b) DPPC with 30% mol ergosterol (Erg), referred to as DPPC/ERG; (c) DPPC with 30% mol cholesterol (Chol), referred to as DPPC/CHOL. All lipid bilayer systems were prepared using CHARMM-GUI Membrane Builder⁵⁴ and embedded in $7.9 \times 7.9 \times 12.3$ nm rectangular boxes. The systems were composed of 196 DPPC (a) or 196 DPPC and 84 Erg/Chol molecules (b and c) and solvated with 15465 water molecules. 47 K^+ and 47 Cl^- ions were added to maintain physiological ionic strength (0.15 M).

Coarse-grained (CG) simulations of spontaneous oligomerization of AmB molecules were performed using the Martini force field (see Fig. S15).⁵⁵ Due to high similarity between the CG representations of cholesterol and ergosterol, 2 model systems were used: (a) pure dipalmitoylphosphatidylcholine (DPPC) referred to as DPPC; (b) DPPC with 30% mol ergosterol (Erg) referred to as DPPC/sterol, again prepared in CHARMM-GUI Membrane Builder. Systems consisted of 32 AmB, 2688 DPPC (a, b) and 1152 Erg (b) molecules were embedded in $30.0 \times 30.0 \times 8.2$ nm rectangular boxes. 27584 Martini polarizable water particles and 320 Na^+ and 320 Cl^- beads were added to solvate the systems and ensure a physiological ionic strength of 0.15 M.

Molecular Dynamics simulations

All atomistic Molecular Dynamics simulations were performed with Gromacs 5.0.4.⁵⁶ The CHARMM36 force field was used for both phospholipids and sterols.⁵⁷ Amphotericin B parameters were based on the CHARMM generalized force field (CGenFF) and reoptimized using the Force Field Toolkit plugin in VMD.^{58,59} Water was represented explicitly using the TIP3P model. The simulations were performed in the NPT ensemble using the v-rescale thermostat with a reference temperature of 325 K and time constant of 5 ps.⁶⁰ The pressure was semiisotropically coupled to the Berendsen barostat with a reference pressure of 1 bar and a

time constant of 2 ps.⁶¹ To integrate the equations of motion, we used the Verlet leap-frog algorithm with a standard time step of 2 fs. Bond lengths were constrained using P-LINCS except for the water molecules, for which the SETTLE algorithm was used.^{62,63} To calculate electrostatic interactions, particle-mesh Ewald (PME) summation was applied with real space cutoff equal to 1.2 nm and Fourier grid spacing of 0.12 nm.⁶⁴ CG simulations were performed with Gromacs 5.0.7 with Martini model version 2.2 for AmB molecules (see SI for details) and version 2.0 for water, lipids and sterols. The v-rescale thermostat with a relaxation time of 1 ps was used to maintain constant temperature of the simulated systems at 325 K. The pressure was semiisotropically coupled with the Parrinello-Rahman barostat and kept constant at 1 bar with a relaxation time of 12 ps and compressibility of $3 \cdot 10^{-4} \text{ bar}^{-1}$. To calculate electrostatic and van der Waals interactions, the potential-shift method was used with a cut-off radius equal to 1.1 nm.

Equilibrium simulations of AmB transmembrane channels

We prepared atomistic models of barrel-stave double length channels consisting of 2N, i.e., of 8, 10, 12, 14, 16, 18, 20, 22 and 24, AmB molecules by (1) repeated rotation of k -th monomer by $\frac{2k\pi}{N}$ about a selected center of geometry to produce a half-pore, (2) duplication of the half-pore, (3) a rotation of the duplicated half-pore by π about the X axis and (4) alignment of the main axes of the two half-pores and adjustment of their spacing along the Z axis.

Channels built in this way were inserted into the hydrophobic core of the membrane, and overlapping lipids and sterols were removed so that the relative proportions of membrane components remained unchanged. The final compositions of the systems were: 196 DPPC and 84 sterols for $N = 4, 5, 6, 7$; 182 DPPC and 78 sterols for $N = 8, 9, 10, 11$; 178 DPPC and 76 sterols for $N = 12$. All prepared systems were subjected to a steepest-descent energy minimization and a 100 ns simulation with AmB atoms positions restrained to equilibrate the system.

Electrical conductance of monovalent ions

To examine the conductivity of AmB channels, we applied the Computational Electrophysiology (CompEL) protocol as implemented in Gromacs.³⁷ The systems were generated by duplication of the original membrane models: shifting the duplicate system along the Z -axis produced two bilayers and two layers of solvent. An imbalance of ion concentrations was introduced between the two water compartments to produce a constant electric field across the membranes. Systems referred to as Im2 contained 48 K^+ and 47 Cl^- ions in one compartment and 46 K^+ and 47 Cl^- in the other, while in the Im6 system 50 K^+ /47 Cl^- and 44 K^+ /47 Cl^- ions were present, respectively. The pore radius parameter was set to 1.5 nm, and both upper and lower extensions of the cylinder were set to 2.0 nm. After ion translocation through the channel, potassium and chloride ions were swapped with a water molecule with a swap attempt frequency of 100 MD steps. Compartment boundaries were defined by the positions of AmB channels inserted into both membranes. The electrostatic poten-

tial $U(z)$ along the Z -axis, required for conductance calculations, was computed using the *gmx density* tool from the Gromacs package. The electric conductance G of single channel was calculated using the formula:

$$G = \frac{I}{U} \quad (2)$$

where $U = U(z_2) - U(z_1)$ is the transmembrane voltage between the two aqueous compartments. I is the ionic current for a single channel recorded over the time interval Δt , calculated as:

$$I = \frac{ne}{k\Delta t} \quad (3)$$

with n being the number of ions passing within Δt , k being number of compartments/channels (2 in our simulations) and e the elementary charge: $1.602 \cdot 10^{-19} \text{ C}$.

Proton conductance

The susceptibility of oligomeric AmB channels to proton translocation *via* the Grothuss mechanism was estimated in post-processing of free energy simulations.⁴⁷ A custom Python script was used to perform a breadth-first recursive search of wires that connect the top and bottom compartment with a uniformly oriented chain of hydrogen bonds. Both water molecules and AmB hydroxyl groups were allowed to partake in wire formation. Short-term memory was introduced to emulate the effect of an oxonium ion being transiently stuck inside the channel. The script and documentation are available online at https://gitlab.com/KomBioMol/proton_wire.

Free energy of the expansion of an AmB channel

To calculate the free energy profiles for the radial expansion of an octameric ($N=8$) AmB channel, we chose the average radius, \bar{r} , as the reaction coordinate. Here, \bar{r} was defined as the average distance between the center of mass of a single AmB molecule and center of the mass of the channel in XY -dimension, averaged over all molecules forming the channel. To produce initial frames for the free energy simulations, a 500 ns steered MD simulations was performed in which \bar{r} was increased up to the value of 1.2 nm using a time-dependent harmonic potential with a force constant of 500 kJ/mol·nm² and at a rate of 2 nm/ μ s. The sampled reaction coordinate interval was divided into 23 windows (from 0.6 to 1.1 nm every 0.025 nm and from 1.1 to 1.2 every 0.05 nm). Subsequently, 2 variants of Umbrella Sampling (US) runs were performed, in the absence (1 μ s per window) and presence (500 ns per window) of a transmembrane potential maintained with the CompEL.³⁷ In the latter case shorter simulation time was compensated by the presence of two physically identical replicas of the AmB channel in each system, thus yielding identical amounts of data. In all US simulations, a time-independent harmonic potential was applied to each AmB molecule with a force constant of 250 kJ/mol·nm². Since the total bias was not a simple function of the reaction coordinate, \bar{r} , but of all individual distances r_i , the free energy profiles were recovered using the multiple Bennett acceptance ratio (mBAR) approach.⁶⁵

We halve also run 4 independent equilibrium simulation without AmB atoms positions restrained and presence of a transmem-

brane potential maintained with the CompEL for $N = 8$ AmB molecules and mean channel radius 0.8 nm. First 3 systems were composed of 182 DPPC and 78 ERG (as used before). In the fourth simulation we removed sterols and replaced DPPC with POPC. All trajectories were 2- μ s long – see Fig.S6

Free energy of ion translocation through the channel

To obtain 1D free energy profiles for the translocation of potassium and chloride ions through an octameric AmB channel, we ran umbrella sampling simulations for an individual K^+ and Cl^- ion. The reaction coordinate was the Z -distance between the center of mass of the double-length channel and the selected ion. First, a 400 ns steered MD simulation was performed to pull the ion along the Z -axis from the channel center (Z -distance of 0.0) into bulk water (Z -distance of 3.15 nm) using a harmonic potential with a force constant of 1000 kJ/mol-nm². The interval between 0.0 and 3.15 nm was divided into 18 equally spaced windows. In each umbrella window, the ion was restrained using a time-independent harmonic potential with a force constant of 500 kJ/mol to produce 250 ns long trajectories. For both steered MD and US runs, we also restrained the XY -distances of individual AmB molecules from the center of mass of the half-pore they belong to at 0.8 nm, so that the structures roughly corresponded to free energy minima along the channel expansion coordinate. We also repeated Umbrella Sampling simulations for the cationic state of AmB, in which the carboxyl moiety of each AmB molecule in each umbrella window was replaced by its protonated analogue. The weighted histogram analysis method (WHAM)⁶⁶ was used to obtain the free energy profiles. Electrostatic energies for additional analyses were obtained using the *gmx energy* utility from the Gromacs package.

To obtain 2D free energy profiles for the simultaneous translocation of two potassium ions through an octameric channel, we modified the above approach by running multiple-walker 2D well-tempered metadynamics. By substituting water molecules with potassium ions and swapping of ion positions, 6 symmetrical initial configurations were generated. Each 1 ps, a 2D Gaussian biasing potential was deposited with standard deviation of 0.05 nm and initial height of 0.3 kJ/mol; the bias factor was set to 10, which corresponded to the “hot” reaction coordinate temperature of 2925 K. The resulting free energy profiles were symmetrized as (a) both ions and (b) both half-channels are in principle chemically identical.

Free energy calculations for the separation of half-channels

The free energy of functional double-length channels formation was estimated using a reaction coordinate ζ defined as the XY -distance between the centers of mass of the two constituent half-pores ($N=2, 4, 6, 8$). In a steered MD simulation, centers of mass of the upper- and lower-leaflet half-pores were pulled away in DPPC/ERG membrane to an XY -distance of 2.55 nm using a time-dependent harmonic potential with a force constant of 5000 kJ/mol and rate $3 \cdot 10^{-6}$ nm/ps. The association pathway

($0 < \zeta < 2.55$) was divided into 18 equally spaced windows, and for all of them 250 ns long trajectories were produced in which ζ was restrained using a time-independent harmonic potential with a force constant of 500 kJ/mol. Windows in DPPC/CHOL were prepared by exchanging ergosterol into cholesterol molecules, while windows in DPPC were obtained by removing sterols and subsequently making short 10 ns simulation with restrained AmB in order to relax the lipid bilayer. In both steered MD and Umbrella Sampling simulations an additional semiharmonic restraint was imposed with a force constant of 1500 kJ/mol to prevent individual AmB molecules from diffusing away more than 0.7 nm from the center of mass of the respective half-pore. Additionally, the same US procedure was carried out by exchanging AmB into its derivative with a deletion of the tail hydroxyl group (35-deoxy AmB). As previously, WHAM was used to obtain free energy profiles, and *gmx energy* utility was used to obtain electrostatic energies.

Amphotericin B model in Martini forcefield

Martini model of AmB molecule was prepared according to Martini guidelines⁵⁵ 4-to-1 mapping was used for the macrocyclic part and 3 beads were used to map the mycosamine moiety (see Fig. S15c). Bonded terms (bond lengths, bond angles, dihedral angles, and their respective force constants) were obtained from distributions derived from a 500-ns long equilibrium simulation of a single AmB molecule embedded in a DPPC bilayer. Non-bonded terms were adjusted to reproduce the free energy profiles for the association of two AmB molecules both in the same leaflet or two opposing leaflets of DPPC-sterol membrane (Fig. S15a, b).

Free energy of amphotericin B dimerization – all-atom simulations

To obtain free energy profiles for the AmB dimerizations, we ran umbrella sampling simulations. The systems were composed of two AmB molecules embedded in a one or two bilayer leaflets, 194 DPPC and 84 Erg molecules, solvated with 15465 water molecules with 47 K^+ and 47 Cl^- anions added to provide physiological ionic strength. The reaction coordinate was the XY -projection of a distance (XY -distance) between centers of mass of single AmB molecules. First, three 500 ns steered MD simulation was performed to pull away AmB monomers using harmonic potentials with a pulling rate 5000 kJ/mol-nm². In case, where AmB monomers was in one membrane leaflet, the interval between 0.6 and 2.3 nm was divided into 18 equally spaced windows (6 from all of 3 steered MD simulations). In each umbrella window, the AmB was restrained using a time-independent harmonic potential with a force constant of 239 kJ/mol to produce 250 ns long trajectories. Same as previous, for AmB placed in opposite leaflets, we divided distance between 0.0 and 1.7 into 18 equally spaced windows (6 from all of 3 steered MD simulations). In all of 18 250 ns trajectories, AmB distance was restrained using a time-independent harmonic potential with a force constant of 59.5 kJ/mol. The weighted histogram analysis method (WHAM)⁶⁶ was used to obtain the free energy profiles.

Free energy of amphotericin B dimerization – coarse-grained simulations

Hamiltonian replica exchange umbrella sampling was used to determine the free energy of AmB dimerization in DPPC-sterol membrane. The systems were composed of two AmB molecules embedded in a bilayer composed of 134 DPPC and 56 Erg molecules, solvated with 2600 water molecules with Na⁺ and Cl⁻ anions added to provide physiological ionic strength. As a reaction coordinate for the association of AmB in one leaflet, a *XY* projection of a distance (*XY*-distance) between centers of mass of AmB molecules was used. Initial configurations for US windows were generated with 40 ns of steered-MD simulation, in which the center of harmonic potential with a force constant of 250 kJ/mol·nm² applied to the *XY*-distance between AmB molecules was moved with a constant velocity from 0.3 nm to 3.3 nm. The distance was then divided into 16 equally spaced windows and

harmonic potential with a force constant of 200 kJ/mol·nm² was used to restrain the *XY*-distance between AmB molecules. The free energy profile for the association of two AmB molecules in opposing leaflets was computed along the *XY*-distance between the beads involving O35 hydroxyl group (O35 bead) of AmB molecules. Initial coordinates for US window were taken from 40 ns long steered-MD simulation, during which O35 beads were pulled towards each other from the initial *XY*-distance of 2 nm to 0 nm, using the harmonic potential with a force constant of 250 kJ/mol·nm². The *XY*-distance interval 0–2 nm was divided into 11 equally spaced windows and in each window the *XY*-distance between O35 beads was restrained using the harmonic potential with a spring constant of 100 kJ/mol·nm². In both cases, 800 ns of simulation was performed for each US window. The free energy profiles were obtained using WHAM and errors were estimated by means of Monte Carlo bootstrap method taking into account autocorrelation of time series.

Table 1 Experimental values of measured AmB channel conductances

Authors	Year	Potential [mV]	Ionic strength	AmB conc. [$\mu\text{M}/\text{ml}$]	Membrane composition	Smallest meas. cond. [pS]
Ermishkin et al. ⁶⁷	1977	200	2M KCl	$0.5 \cdot 10^{-7}$	PC:CHOL (2:1)	6.5
Ostroumova et al. ¹³	2012	200	2M KCl	10^{-6}	PC:CHOL (2:1)	7.0
Cotero et al. ¹⁶	1998	200	2M KCl	10^{-6}	DMPC:CHOL (7:3)	1.6
Venegas et al. ⁸	2003	200	2M KCl	10^{-6}	DMPC:CHOL (7:3)	3.9

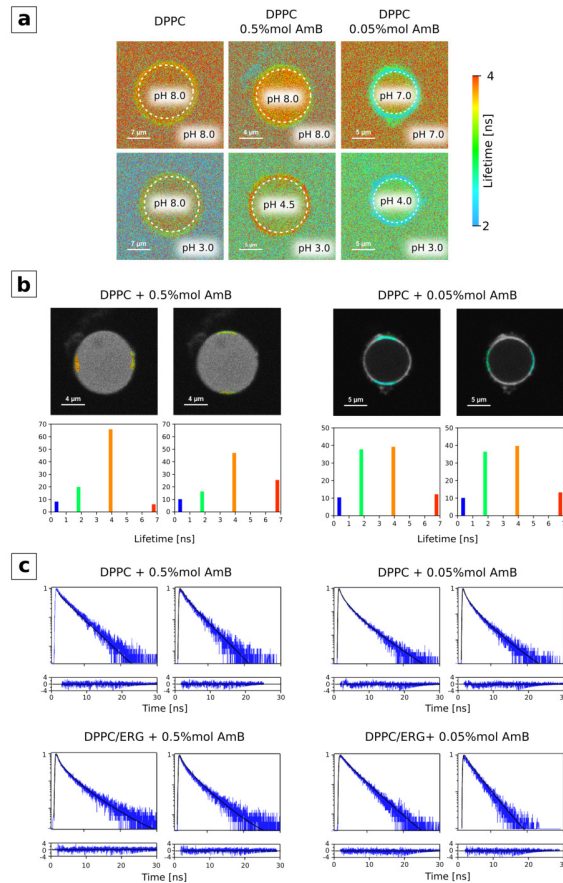


Fig. S1 (a) pH values in GUVs composed of DPPC, DPPC with 0.5%M AmB and DPPC with 0.05%M AmB, recorded before (upper panel) and after (lower panel) acidification with HCl. (b) Top panel: fluorescence lifetime imaging of photoselcted AmB molecules oriented vertically (right and left side of the GUV) and horizontally (top and bottom of the GUV) with respect to the membrane plane. Bottom panel: Distribution of fluorescence lifetimes for the corresponding AmB orientations. The panel is analogous to Fig. 2b but shows results for sterol-free (DPPC/AmB) systems. (c) Raw fluorescence decay curves for which the four-exponential fitting was performed to quantify individual lifetime components in panel (b).

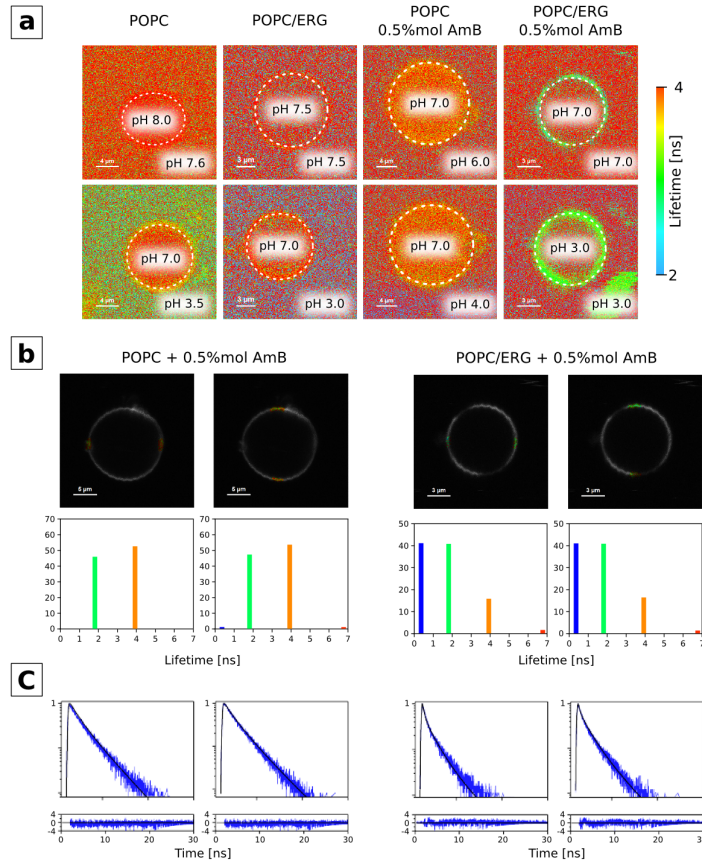


Fig. S2 (a) pH values in GUVs composed of POPC, POPC/ERG, POPC with 0.5%M AmB and POPC/ERG with 0.5%M AmB, recorded before (upper panel) and after (lower panel) acidification with HCl. (b) Top panel: fluorescence lifetime imaging of photoselected AmB molecules oriented vertically (right and left side of the GU) and horizontally (top and bottom of the GU) with respect to the membrane plane. Bottom panel: Distribution of fluorescence lifetimes for the corresponding AmB orientations. (c) Raw fluorescence decay curves for which the four-exponential fitting was performed to quantify individual lifetime components in panel (b).

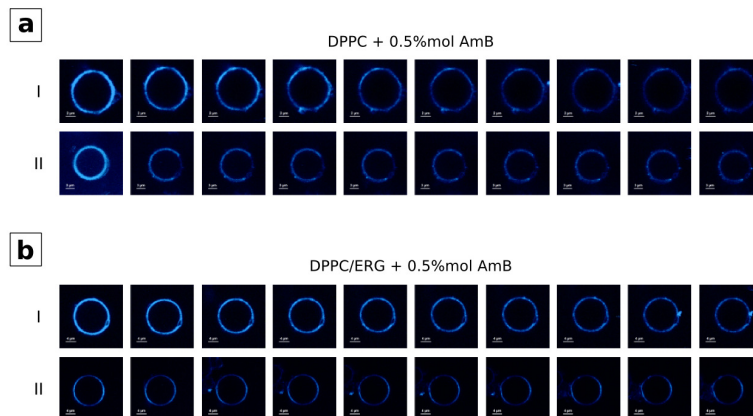


Fig. S3 Fluorescence intensity decay due to oxidative bleaching observed in liposomes composed of DPPC (a) or DPPC/ERG (b) with 0.5%M AmB. Sodium dithionite was added after (I) or during (II) electroformation. Fluorescence intensities are plotted in Fig. 2c.

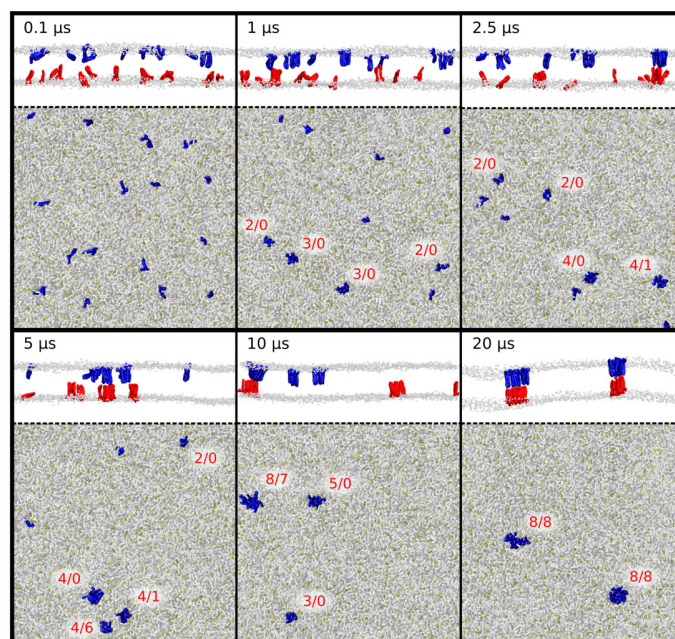


Fig. S4 Spontaneous oligomerization of AmB molecules in 20 μ s coarse-grained simulation. In six snapshots from a representative run, the figure shows the oligomers in the upper (blue) and lower (red) membrane leaflet along with a number of particles constituting the oligomer.

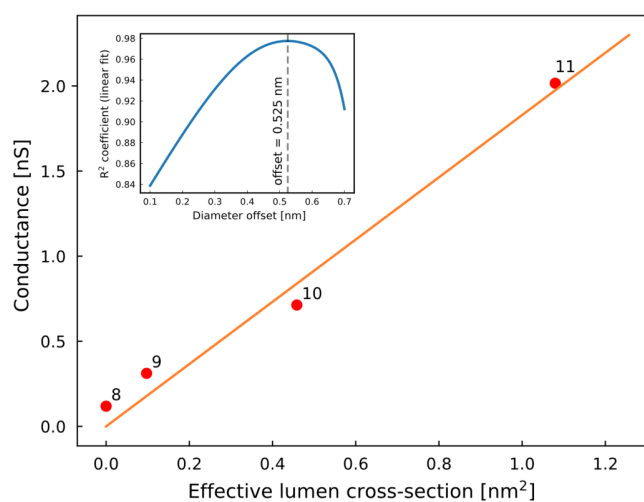


Fig. S5 Conductance of the restrained DLCs as a function of an effective channel lumen cross-section. An optimal offset for the solvated ion diameter was chosen so as to maximize the determination coefficient in the linear fit of conductance vs. effective cross-section. The HOLE program was used to calculate the minimal channel radii.

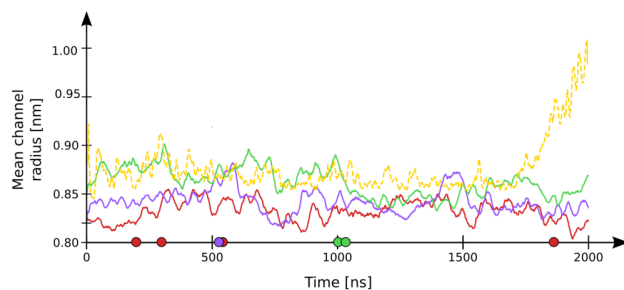


Fig. S6 Evolution of the mean channel radius during four independent 2- μ s computational electrophysiology simulations of the octameric (N=8) DLC (1-red, 2-violet, 3-green, 4-yellow). First 3 simulations (solid lines) were performed for the channel embedded in DPPC/ERG and the last one (dashed line) in POPC (see Methods). Transitions of potassium ions are marked with dots; no transitions were observed for the POPC-embedded channel.

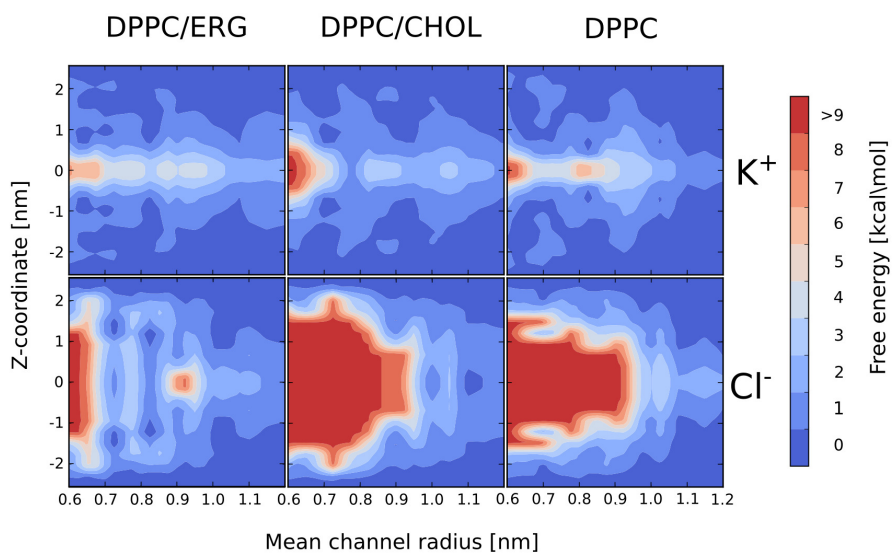


Fig. S7 Symmetrized 2D free energy map for potassium and chloride ions as a function of the mean channel radius and the Z-coordinate. The free energies were calculated by Boltzmann inversion of histograms obtained from the channel extension simulations. Regions never visited in the simulations are marked in dark red.

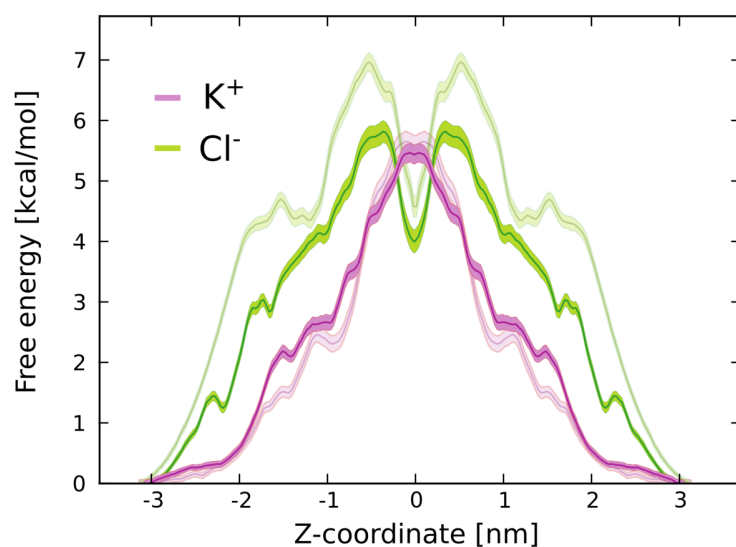


Fig. S8 Free energy profiles for K^+ and Cl^- passing through an octameric DLC composed of cationic AmB (see Methods) in the absence of a transmembrane potential. The corresponding profiles for zwitterionic AmB are shown as semitransparent.

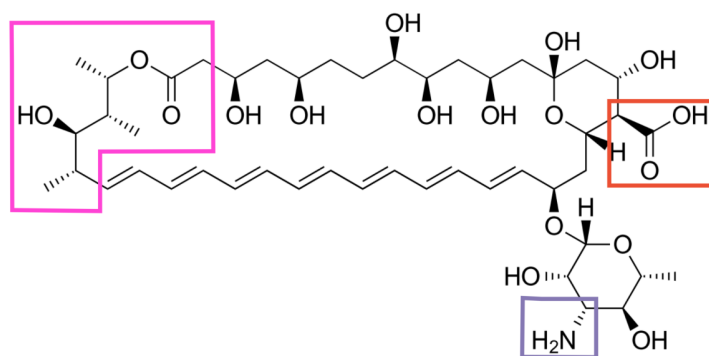


Fig. S9 Key chemical moieties within an AmB molecule that were used for energy decomposition in Fig. 6b: the carboxyl group (red), the amine group (violet) and the tail region (pink). The remaining part is labeled as "AmB". Thus defined groups have net charges of -1, 1, 0 and 0, respectively.

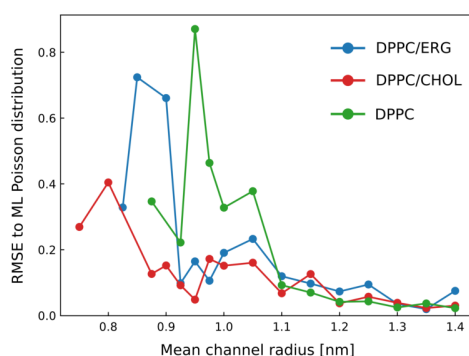


Fig. S10 Similarity of the distribution of ion passage waiting times observed in the computational electrophysiology simulations to the Poisson distribution. A maximum likelihood approach was used to estimate model parameters, and RMSE was calculated between the observed data (time-normalized) and a canonical Poisson distribution at different values of the mean channel radius. As a result, low RMSE values are indicative of uncorrelated ion passage events.

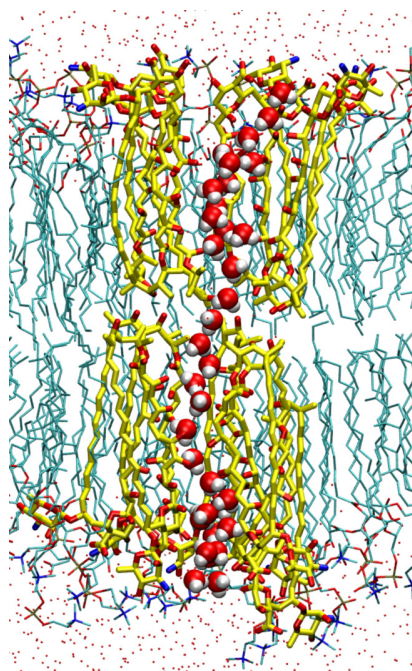


Fig. S11 Snapshot of a sample „proton wire” encountered during the proton conductivity analysis. A continuous, ordered path of hydrogen-bonded water molecules can be traced from the top to the bottom of the channel.

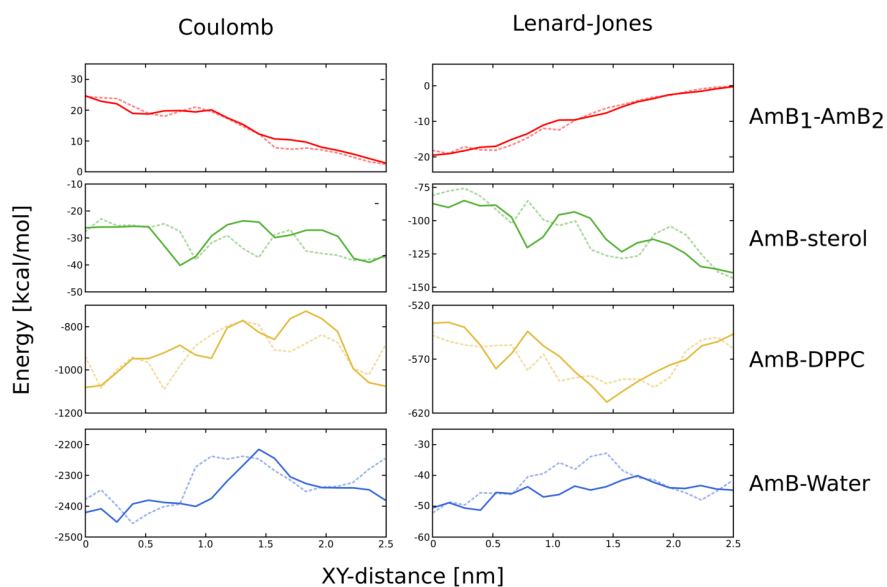


Fig. S12 Coulombic and vdW contributions to the interaction energy between (1) the two AmB halfpores (N=8), (2) AmB and sterols, (3) AmB and DPPC and (4) AmB and water as a function of XY-distance between the two halfpores' centers of mass.

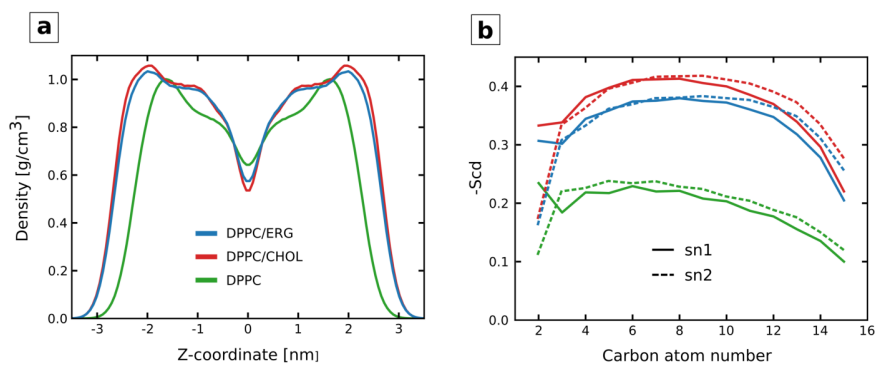


Fig. S13 (a) Density profiles for the three lipid bilayer used in our fully atomistic simulations. (b) Order parameter ($-S_{cd}$) profiles for the two phospholipid acyl chains, sn1 (solid line) and sn2 (dashed line), in the three lipid bilayers used in our fully atomistic simulations.

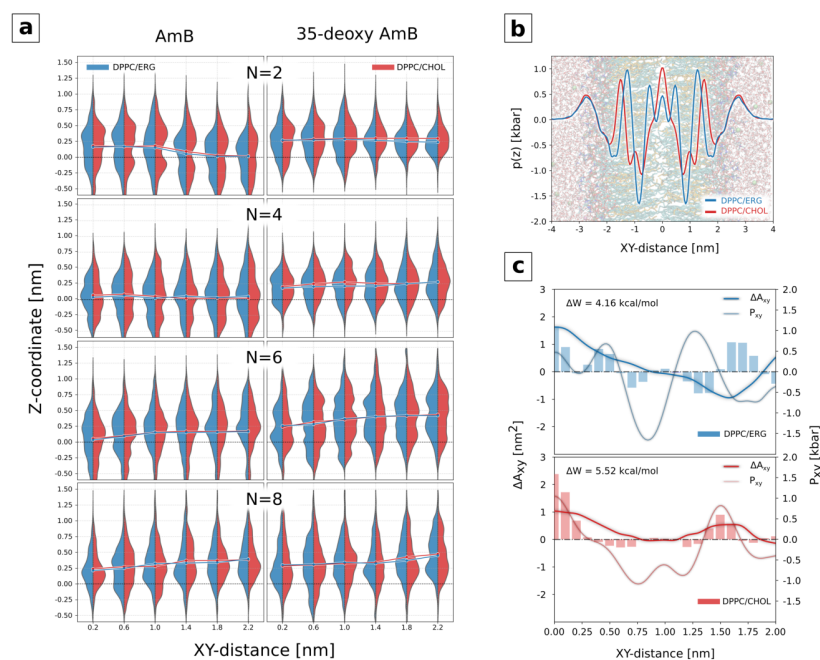


Fig. S14 (a) Violin plots showing the distribution of Z -coordinate of the molecule's tail region during the descent of two dimeric, tetrameric, hexameric and octameric half-channels composed of AmB (left) and 35-deoxy AmB (right). On top of the distributions, solid lines mark average values. Results are shown for two membrane systems, ergosterol- and cholesterol-rich (blue and red, respectively). (b) Lateral pressure profiles for the two sterol-rich membranes: DPPC with 30%mol ergosterol (blue) and DPPC with 30%mol cholesterol (red), in absence of AmB. (c) Lateral pressure (thin line) plotted against changes in XY -plane cross-section area during the descent of two octameric halfpores (thick line). Bars visualize the product of the two, i.e., contributions to the work performed against the lateral pressure during half-pore descent was 4.16 and 5.52 kcal/mol in DPPC/ERG/AmB and DPPC/CHOL/AmB systems, respectively.

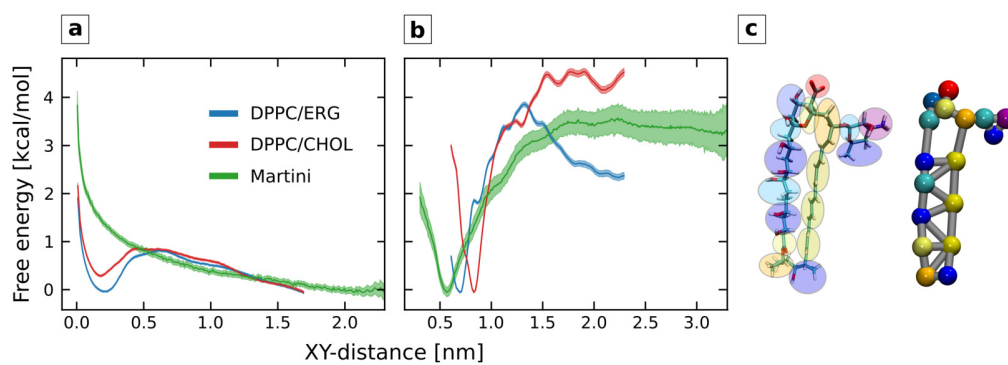


Fig. S15 Free energy profiles for the dissociation of two AmB monomers in one (a) and two (b) membrane leaflets in all-atom (red and blue) and coarse-grained (green) simulations. (c) Mapping of the Martini beads onto an atomic structure of AmB.